Continuum model for inelastic behaviour of masonry

Luca Pelà[1], Miguel Cervera[2], Pere Roca[2]

[1]*DICAM Department, University of Bologna, Italy*
E-mail: *luca.pela@unibo.it*

[2]*Technical University of Catalonia, Barcelona, Spain*
E-mail: *miguel.cervera@upc.edu; pere.roca.fabregat@upc.edu*

Keywords: viscoelasticity, orthotropy, tensile crack localization.

SUMMARY. A continuum model capable of modelling the inelastic behaviour of masonry is presented. The model includes the description of viscoelasticity, orthotropic damage and tensile crack localization. The theoretical framework is summarized. The model has been implemented in a FE package and validated through the analysis of a complex masonry construction and the simulation of experimental tests on shear walls.

1 INTRODUCTION

This work presents a theoretical framework for continuum modelling of masonry structures. The material is described at the macro-level, i.e. it is modelled as a homogeneous continuum [1]. Closed-form macro-models represent a possible option to produce efficient structural computations [2-3]. The constitutive law is based on Continuum Damage Mechanics and describes inelastic behaviours under tension, compression or shear stress states. The proposed framework is also suitable for including the description of time-dependent phenomena, such as viscous effects and creep. The description of orthotropic behaviour can be simulated resorting to the concept of mapped tensor from the anisotropic field to an auxiliary workspace [4]. The application of this idea to strain-based Continuum Damage Models is innovative and leads to several computational benefits [5-6].

The finite-element method is adopted as a framework for numerical implementation. The tensile damage propagation is modelled through standard finite elements and a crack-tracking technique [7] which represents localized-discrete cracks, similar to the ones typically observed on masonry structures. Compared with the smeared approach, the localized model shows a better capacity to predict the real collapsing mechanism and leads to mesh objective results.

The suitability of the model for representing the behaviour of masonry elements is shown via the simulation of experimental tests. The possibility of using the proposed numerical model to study complex constructions is also investigated.

2 VISCOELASTICITY MODEL

The rheological model can be schematized through the Maxwell's chain shown in Figure 1. The first chain element is composed by a spring with elastic stiffness E_∞, whereas the second element is composed by a spring with elastic stiffness E_v, arranged in series with a dashpot with a viscosity parameter η. The springs response is linear elastic whereas the viscous stress in the dashpot is proportional to the viscous strain rate.

The initial stiffness of the system is given by the sum of the stiffnesses of the two springs, being the dashpot of the Maxwell's chain infinitely stiff at the beginning of the deformation

process. Thus, the instantaneous elastic modulus E can be defined as follows:

$$E = E_\infty + E_v \tag{1}$$

The stiffness of the system for $t = +\infty$ is equal to E_∞, since the dashpot is completely slackened at the end of the deformation process. The total stress sustained by the Maxwell's chain is given by the sum of the stresses in the two elements:

$$\sigma = E_\infty \varepsilon + \xi E\left(\varepsilon - \varepsilon_v\right) \tag{2}$$

in which $\xi = E_v / E$ is the participation ratio which denotes the amount of stiffness susceptible to viscosity. The total deformation of the system is denoted by ε, whereas ε_v denotes the viscous strain of the chain which increases with time under a constant stress σ. The phenomenological behaviour of the model is depicted in Figures 1b-d, which also show the effect of the so-called retardation time $\theta = \eta / E_v$ on the time-dependent increase of strain or decrease of stiffness.

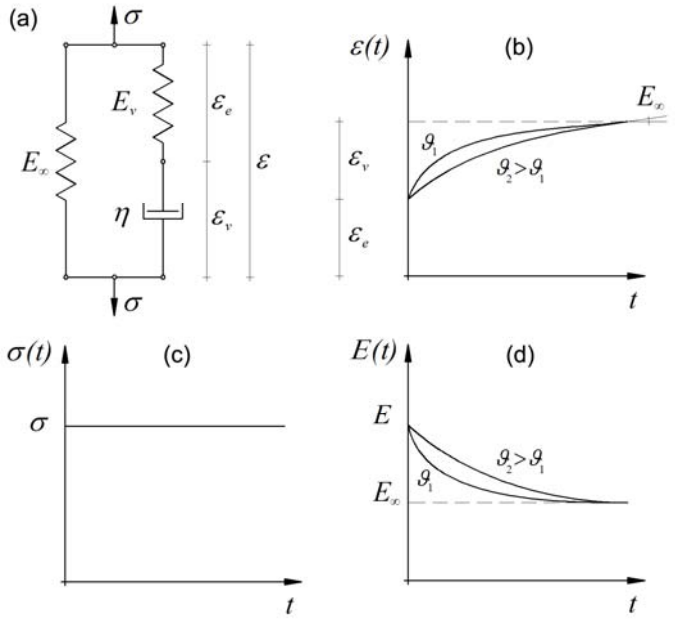

Figure 1: Viscoelasticity model: a) schematization through a Maxwell chain and strain (b), stress (c) and stiffness (d) time-dependent laws.

The strain rate of the system is defined by the following equation:

$$\dot{\varepsilon} = \frac{\dot{\sigma}_v}{E_v} + \frac{\sigma_v}{\eta} \tag{3}$$

Thus, the first order differential equation governing the evolution of the viscous stress is given by:

$$\xi E\dot{\varepsilon} = \dot{\sigma}_v + \frac{\sigma_v}{\vartheta} \tag{4}$$

The previous equation can be rewritten for the multidimensional case, using the tensorial counterparts of the scalar terms used for the uniaxial model:

$$\xi \mathbf{C}\dot{\boldsymbol{\varepsilon}} = \dot{\boldsymbol{\sigma}}_v + \frac{\boldsymbol{\sigma}_v}{\vartheta} \tag{5}$$

With the aim of assuming the viscous strain in the Maxwell's chain as internal variable, the relationship

$$\boldsymbol{\sigma}_v = \xi \mathbf{C}\left(\boldsymbol{\varepsilon} - \boldsymbol{\varepsilon}_v\right) \tag{6}$$

can be included in Equation (5), leading finally to the evolution law for the viscous strain:

$$\dot{\boldsymbol{\varepsilon}}_v = \frac{1}{\vartheta}\left(\boldsymbol{\varepsilon} - \boldsymbol{\varepsilon}_v\right) \tag{7}$$

The solution of the differential equation for a generic time step t_{n+1} can be obtained by integrating the previous equation, leading finally to [8]

$$\boldsymbol{\varepsilon}_v\left(t_{n+1}\right) = \boldsymbol{\varepsilon}_v\left(t_n\right) + \frac{\Delta t}{\vartheta}\left[\boldsymbol{\varepsilon}\left(t_{n+1}\right) - \boldsymbol{\varepsilon}_v\left(t_n\right)\right] \tag{8}$$

3 ORTHOTROPIC DAMAGE MODEL

Masonry orthotropic behaviour can be simulated by means of an original methodology, which has been recently proposed in Refs. [4-5] for CDM models. It is based on establishing a conveniently defined mathematical relationship (called "mapping") between the anisotropic space and a scaled isotropic one. In this way, it is possible to solve the problem in scaled space and to return the results to the anisotropic field. This strategy allows one to take advantage of all the benefits related to the use of isotropic models, especially in terms of simplicity and computational efficiency.

The mapping relationship between the anisotropic and the scaled isotropic space is defined by means of two transformation tensors $\mathbf{A}^{\sigma}$ and $\mathbf{A}^{\varepsilon}$, which are related to stress and strain components, respectively:

$$\boldsymbol{\sigma}^{*} = \mathbf{A}^{\boldsymbol{\sigma}} : \boldsymbol{\sigma} \tag{9}$$

$$\boldsymbol{\varepsilon}^{*} = \mathbf{A}^{\boldsymbol{\varepsilon}} : \boldsymbol{\varepsilon} \tag{10}$$

A general quantity is denoted by a superscripted (*) if it is related to the scaled space. The four rank-transformation tensors defines a bijective linear transformation between the real anisotropic and the scaled isotropic spaces, see Figure 2.

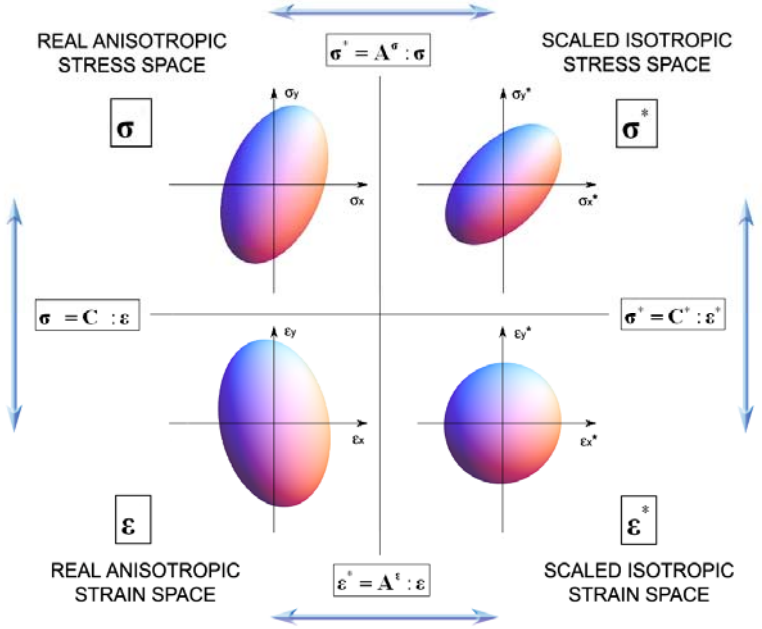

Figure 2: Mapping relationship between the real anisotropic and the scaled isotropic spaces [4].

Tensor components can be selected in order to obtain a favourable auxiliary workspace for the numerical procedure to be adopted. In this work, a simple scaling of stress components is sufficient to reproduce elastic and strength orthotropy of the material. Therefore, the non-null components of the stress transformation tensor can assume the following form in two-dimensional plane stress conditions:

$$\begin{aligned} A^{\sigma}_{1111} &= f^{*}_{11} / f_{11} \\ A^{\sigma}_{2222} &= f^{*}_{22} / f_{22} \\ A^{\sigma}_{1212} &= A^{\sigma}_{1221} = A^{\sigma}_{2112} = A^{\sigma}_{2121} = f^{*}_{12} / \left(2 f_{12}\right) \end{aligned} \tag{11}$$

where f_{ij} and f_{ij}^{*} are the real (orthotropic) and scaled strengths, respectively. In order to reproduce an isotropic failure criterion in the scaled space, it suffices that $f_{11}^{*} = f_{22}^{*} = f^{*}$. The choice of f^{*} is arbitrary. The expression of f_{12}* depends on the particular isotropic criterion adopted.

The strain space transformation tensor in matrix form results after simple calculations [4]:

$$\mathbf{A}^{\varepsilon} = \left(\mathbf{C}^{*}\right)^{-1} : \mathbf{A}^{\sigma} : \mathbf{C} \tag{12}$$

where **C** and **C*** are the orthotropic and the isotropic linear constitutive tensors, respectively.

The tension-compression damage model [9] is considered to solve the mechanical problem in the scaled space. Such model is based on a split of the effective stress tensor $\bar{\boldsymbol{\sigma}}^{*}$ [10] into tensile and compressive components, $\bar{\boldsymbol{\sigma}}^{+*}$ and $\bar{\boldsymbol{\sigma}}^{-*}$, in order to account for different material behaviour in tension and compression. Once defined the internal damage variables d^{+} and d^{-}, each related with

the sign of the stress and thus with tension and compression, the constitutive equation takes the form:

$$\boldsymbol{\sigma}^{*} = \left(1 - d^{+*}\right)\overline{\boldsymbol{\sigma}}^{+*} + \left(1 - d^{-*}\right)\overline{\boldsymbol{\sigma}}^{-*} \tag{12}$$

The internal damage variables are equal to zero when the material is undamaged and equal to one when it is completely damaged [10].

On the basis of the aforementioned assumptions, it is evident that the mapping procedure allows us to scale sensibly the desired orthotropic criterion into a convenient isotropic computation space. Since masonry presents different mechanical behaviour under tensile or compressive states, it is possible to carry out two distinct mappings for tensile and compressive stresses $\boldsymbol{\sigma}^{+*}$ and $\boldsymbol{\sigma}^{-*}$, making use of two stress transformation tensors $\mathbf{A}^{\sigma+}$ and $\mathbf{A}^{\sigma-}$.

In this work, a Rankine criterion is assumed in the scaled space for tensile stress contributions while for compressive ones the Drucker-Prager based criterion proposed by Faria et al. [11] is used. Such choices correspond implicitly to an orthotropic composite failure surface in the original anisotropic space, able to fit accurately any set of experimental data on orthotropic masonry [1,4-5], see for instance Figure 3.

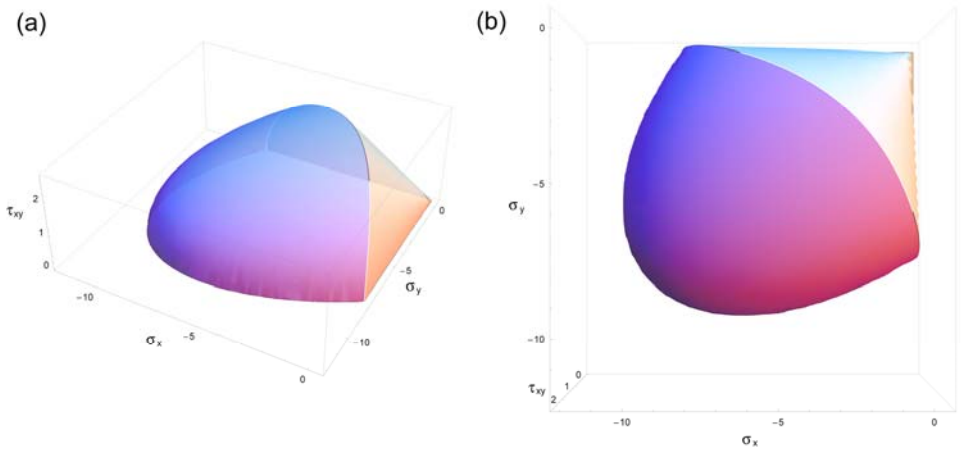

Figure 3: Failure surfaces for solid clay brick masonry according to Page's experimental tests [5].

Concerning the description of the material response in the non linear range, the post-peak behaviour is defined by means of the material fracture energies in tension and compression $G_f^{\pm *}$. These parameters are normalized with respect to the finite element characteristic length, in order to ensure FEM solution mesh-independency [12]. An exponential softening law is used for tension, whereas a hardening branch followed by exponential softening is assumed for compression.

4 TENSILE CRACK LOCALIZATION

The classical smeared crack approach, based on CDM and standard finite elements, is not able to simulate individual discrete cracks under tensile stresses. This is due to the inability of this approach to reproduce accurately the near-singular strain and stress fields in the tip of the progressing cracks [13-15]. Such limitation is overcome in this work adopting the local crack-

tracking technique proposed in Ref. [7], which forces the tensile crack to develop along a single row of finite elements. The fracture energy normalization with respect to the characteristic length ensures that dissipation will be element-size independent [12].

The proposed method is applied at every time step during the FE analysis, just before the stress evaluation. The method uses a flag system, where finite elements are labelled to delimit the zones where cracks will appear or develop. The criteria used to define these zones depend on the magnitude and direction of the principal stresses at each element (Figure 4). The algorithm ensures mesh-bias and element-size objective FE results and has been implemented for 2D problems using three-noded triangular elements.

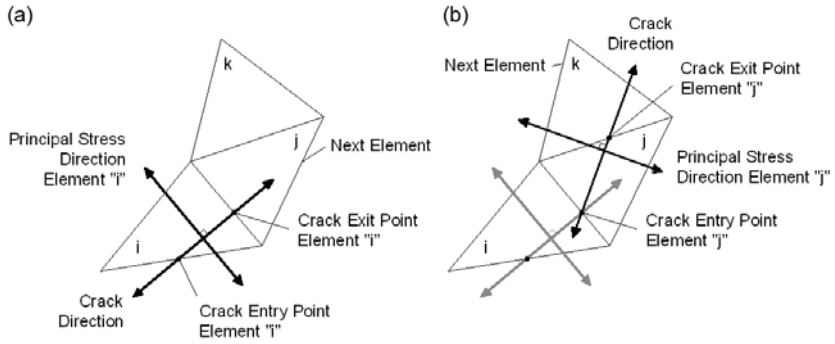

Figure 4: Crack-tracking technique [7]: operation for element *i* (a) and following element *j* (b).

5 NUMERICAL EXAMPLES

The viscoelasticity and tension-compression models, the mapping procedure and the crack-tracking technique have been implemented into the FE program COMET [16] developed at the International Centre for Numerical Methods in Engineering (CIMNE, Barcelona). Two numerical applications are presented in the following: the simulation of Mallorca Cathedral typical bay and the analysis of experimental tests of shear walls. Pre- and post-processing have been carried out with GiD [17], also developed at CIMNE.

5.1 *Simulation of the construction process of Mallorca Cathedral typical bay*

The construction process of Mallorca Cathedral typical bay has been simulated numerically resorting to a finite element activation technology able to reproduce the addition of different structure portions during the building stages. This strategy classifies the elements of the FE mesh into active and inactive. At the beginning of the analysis, the elements which define the first portion built are activated, i.e. computed and assembled into the global matrix, whereas the inactive elements are disregarded in calculations. In the following step, the elements corresponding to the next construction stage are activated and the calculation proceeds, considering the first portion already deformed. By repeating such procedure until the completion of all building stages, it is possible to obtain a numerical simulation of the whole construction process.

Three groups of materials have been distinguished for different structural members. The first includes buttresses, vaults, ribs and clerestory, whose properties were assumed as follows: Young's modulus E=2000 MPa, Poisson's ratio v=0.2, tensile and compressive strengths f^+=0.1 MPa and f^-=2 MPa. The second group includes columns, flying arches, with E=8000 MPa,

ν=0.2, f^+=0.4 MPa and f^-=8 MPa. The properties of the material of the central vault backing are E=1000 MPa, ν=0.2, f^+=0.05 MPa and f^-=1 MPa. Reasonable values for the fracture energies have been assumed for all materials (G_f^+=100 J/m^2, G_f^+=40000 J/m^2), since they were not measured experimentally. The retardation time is assumed arbitrarily as θ=50 time units. Its effective entity is not significant and has to be related only to the total number of time steps in calculations. Concerning the participation ratio, two different values have been considered, ξ=0.875 and ξ=0.975, in order to assess the variability of results. These assumed values are great enough to analyse the structure under extremely adverse conditions, since they presume that a great amount of stiffness is susceptible to creep. The hypothesis of geometric nonlinearity has been assumed, through a total Lagrangian formulation with the assumption of small-strain/large-displacement.

The numerical simulation of the construction process consists of three subsequent analysis steps, in compliance with the information about the building stages provided by the historical investigation [18]. In the first step (see Figure 5a), the pier, the aisle vault and the buttress are activated in the FE model. In the second analysis step (see Figure 5b), the upper part of the buttress, the flying arches, the clerestory, the nave vault are subsequently activated and the calculus is carried on starting from the stress-strain state obtained at the end of first analysis. Finally, the structure is subject to constant loading and the time starts elapsing in order to evaluate the deformation accumulation due to creep (see Figure 5c).

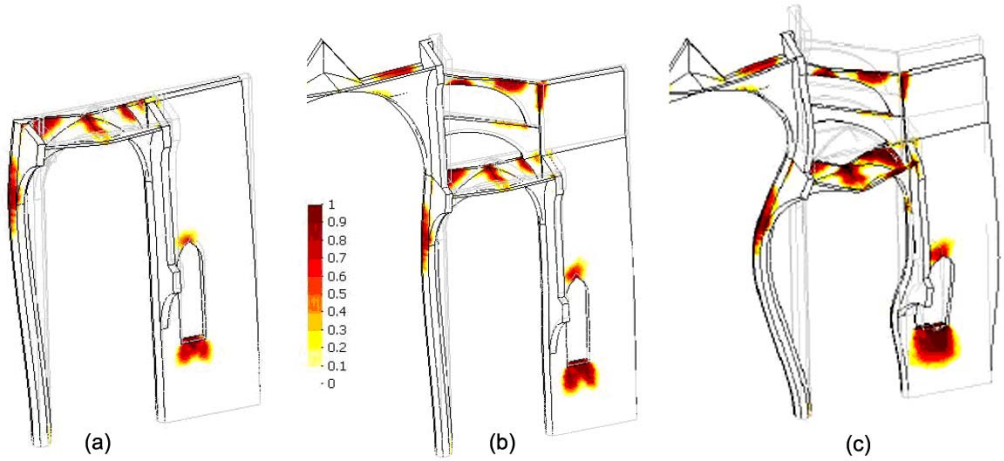

Figure 5: Tensile damage in Mallorca Cathedral typical bay after the stages of construction (a-b), and due to material creep (c).

Figure 6 shows the horizontal displacements evolution at pier top due to creep. In case of ξ=0.875, the pier top horizontal time-dependent displacement reaches a stable value of 12 cm after 3,000 time units. This order of magnitude is comparable to the real displacements recently measured in Mallorca Cathedral bays [19], showing the concrete possibility that creep phenomena and geometric effects had played a significant role during the life of the structure. It is worth noticing that a conventional instantaneous analysis of the cathedral bay, i.e. without resorting to the construction process simulation with viscoelasticity model and geometric nonlinearity, would have led erroneously to a horizontal displacement at the pier top of only 0.76 cm.

The assumptions of geometric nonlinearity and ξ=0.975 lead to the simulation of the structure collapse, as shown by the corresponding curve in Figure 6 at 2,000 time units. It can be concluded that the numerical simulation can represent the failure condition only for extremely high values of

the participation ratio. Therefore, it seems unlikely that Mallorca Cathedral can collapse for long-term creep phenomena under the gravitational loads.

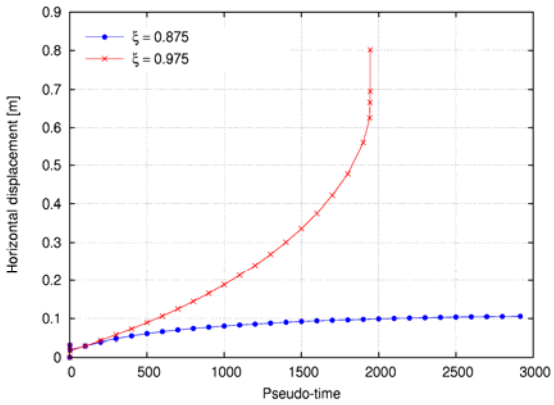

Figure 6: Horizontal displacement increase at pier top due to creep.

5.2 *Simulation of experimental tests on shear walls*

The experiments carried out on shear walls with a central opening by Raijmakers and Vermeltfoort [20] are here considered. The walls denoted J2G and J3G have been chosen for this purpose. Vertical precompression uniformly distributed forces p = 0.30 N/mm^2 are applied to the walls, before a horizontal load is monotonically increased under top displacement control d in a confined way, i.e. keeping the bottom and top boundaries horizontal and precluding any vertical movement.

The values of the mechanical parameters used in the numerical analysis to describe the masonry behaviour are the following: E_1=E^*=7520 MPa, E_2=3960 MPa, ν_{12}=ν^*=0.09, ν_{21}=0.05, G_{12}=1460 MPa, f_{11}^+=f^{+*}=0.35 MPa, f_{22}^+=0.25 MPa, f_{12}^+=0.30 MPa, f_{11}^-=f^{-*}=6.30 MPa, f_{22}^-=4.50 MPa, f_{12}^-=3.0 MPa, $G_{f,1}^-$=G^{-*}=20000 J/m^2 and $G_{f,2}^-$=19400 J/m^2.

The comparison between the calculated and experimental load-displacement diagrams is shown in Figure 7. The results agree reasonably well, both in the elastic field and in the inelastic one. This indicates that the deformability of the wall as well as the failure mechanism are properly represented.

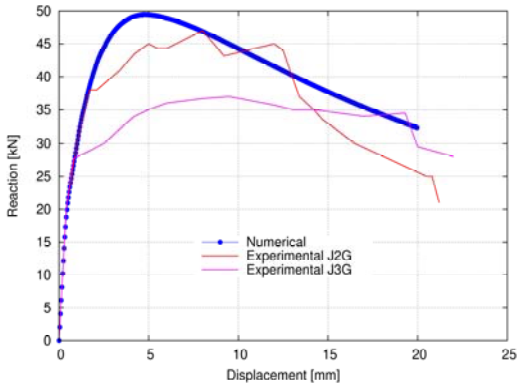

Figure 7: Walls J2G and J3G. Load vs. displacement diagrams.

Figure 8a illustrates the tensile damage contour. The experimental behaviour is well replicated by the numerical model which represents correctly the cracks opening that cause the global failure mechanism. As shown, the damage in the ultimate conditions is represented in the form of discrete cracks, thanks to the tracking technique which allows tensile cracks to localize. Figure 8b shows the tensile damage contour obtained by a finite element analysis with a traditional smeared damage approach. As shown, the damage spreads unrealistically. The comparison with Figure 8a points out a very important issue. Although it seems that almost the same result has been obtained, the smeared model is considerably mesh-bias dependent: the crack follows a favourable path given by the spatial discretization. This would imply loss of solution objectivity when different alignments of the mesh were considered in the discrete problem.

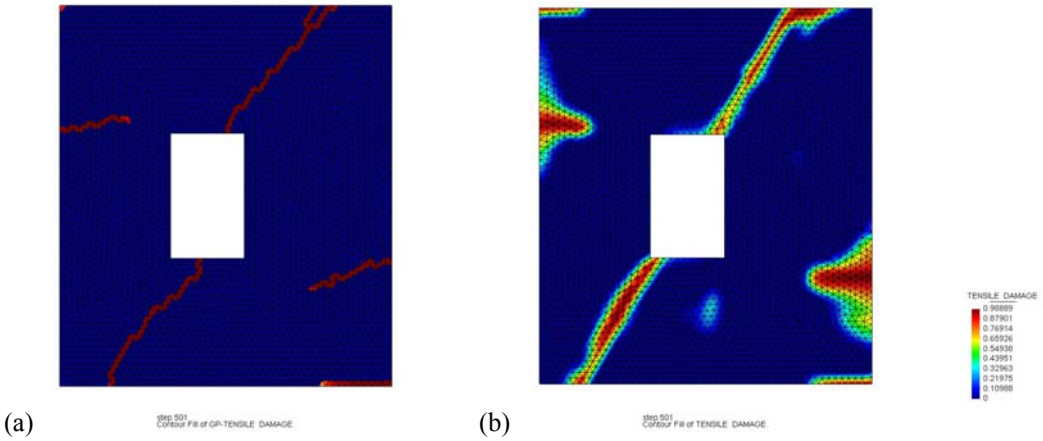

(a) (b)

Figure 8: Tensile damage contour: localized (a) vs. smeared damage (b).

6 CONCLUSIONS

This work has presented a continuum model for the inelastic behaviour of masonry. The model describes the viscoelastic behaviour, the occurrence of orthotropic damage and tensile crack localization. The model has been calibrated through the simulation of experimental tests on shear walls. The numerical study of the construction process of Mallorca Cathedral typical bay has shown the capability of the model of producing realistic and efficient structural computations.

References

[1] Pelà, L., *Continuum Damage Model for Nonlinear Analysis of Masonry Structures*, PhD-Thesis, Technical University of Catalonia, University of Ferrara (2009).

[2] Roca, P., Cervera, M., Gariup, G. and Pelà, L., "Structural analysis of masonry historical constructions. Classical and advanced approaches. *Archives of Computational Methods in Engineering*, **17**, 299–325 (2010).

[3] Pelà, L., Aprile, A. and Benedetti A., "Seismic assessment of masonry arch bridges", *Engineering Structures*, **31**, 1777-1788 (2009).

[4] Pelà, L., Cervera, M. and Roca, P., "Continuum damage model for orthotropic materials: Application to masonry", *Computer Methods in Applied Mechanics and Engineering*, **200**, 917–930 (2011).

[5] Pelà, L., Cervera, M. and Roca, P., "An orthotropic damage model for the analysis of masonry structures", *Construction and Building Materials*, accepted for publication (2011).
[6] Pelà, L., Cervera, M. and Roca, P., "FEM Analysis of Orthotropic Masonry Walls via Localized Damage Models", in *Proc. 8th International Masonry Conference* (CD-ROM), Dresden, Germany, July 4-7, 2010.
[7] Cervera, M., Pelà L., Clemente, R. and Roca, P., "A crack-tracking technique for localized damage in quasi-brittle materials", *Engineering Fracture Mechanics*, **77**, 2431-2450 (2010).
[8] Cervera, M., *Viscoelasticity and rate-dependent continuum damage models*, CIMNE, Barcelona (2003).
[9] Cervera, M., Oliver, J. and Faria, R., "Seismic evaluation of concrete dams via continuum damage models", Earthquake Engineering & Structural Dynamics, **24**, 1225–1245 (1995).
[10] Lemaitre, J. and Chaboche, J.L., "Aspects phénoménologiques de la rupture par endommagement", *J. Méc. Appl.*, **2**, 317–365 (1978).
[11] Faria, R., Oliver, J. and Cervera, M., "A Strain-Based Plastic Viscous-Damage Model for Massive Concrete Structures", *International Journal of Solids and Structures*, 35, 1533-1558 (1998).
[12] Bazant, Z.P. and Oh, B.H., "Crack band theory for fracture of concrete", *Mater. Struct.*, **16**, 155–177 (1983).
[13] Cervera, M., Chiumenti, M., and Codina, R., "Mixed stabilized finite element methods in nonlinear solid mechanics: Part I: Formulation", *Computer Methods in Applied Mechanics and Engineering*, **199**, 2559-2570 (2010).
[14] Cervera, M., Chiumenti, M., and Codina, R., "Mixed stabilized finite element methods in nonlinear solid mechanics: Part II: Strain Localization", *Computer Methods in Applied Mechanics and Engineering*, **199**, 2571-2589 (2010).
[15] Cervera, M., Chiumenti, M., and Codina, R., "Mesh objective modeling of cracks using continuous linear strain and displacement interpolations", *International Journal for Numerical Methods in Engineering*, DOI: 10.1002/nme.3148 (2011).
[16] Cervera, M., Agelet de Saracibar, C. and Chiumenti, M, *COMET: COupled MEchanical and Thermal analysis. Data Input Manual Version 5.0*, CIMNE, Barcelona (2002).
[17] http://gid.cimne.upc.es/, website of CIMNE, Technical University of Catalonia, Barcelona.
[18] Domenge J, *L'obra de la Seu. El procés de construcció de la catedral de Mallorca en el tres-cents* (in Catalan), Palma de Mallorca (1997).
[19] Roca, P. and González, JL, *Estudio, diagnóstico y peritación y en su caso planteamiento de actuaciones sobre el comportamiento constructivo-estructural de la catedral de Santa María, en la ciudad de Palma, isla de Mallorca, Baleares* (in Spanish). Technical University of Catalonia, Barcelona (2008).
[20] Raijmakers, T.M.J. and Vermeltfoort, A.Th., *Deformation controlled tests in masonry shear walls* (in Dutch), research report B-92-1156, TNO-Bouw, Delft (1992).